Proceedings of the
Annual Stability Conference
Structural Stability Research Council
Atlanta, Georgia, April 21-24, 2026

The residual bearing capacity of corroded steel I-beams and their failure patterns

Ashritha Veeramalla[1], Lakshmi P. Subramanian[2]

Abstract

This paper emphasizes the implications of corrosion on the web bearing capacity, highlighting how section loss at girder ends can lead to local buckling and crippling, severely diminishing bearing strength. Corrosion is a predominant factor contributing to the deterioration of steel beams, adversely affecting geometric properties such as section modulus and slenderness ratio. Consequently, this deterioration significantly compromises the load-carrying capacity of structural members across tension, compression, flexure, bearing, and fatigue scenarios. Moisture accumulation at critical junctions, particularly at the bottom web-flange interface, serves as a catalyst for corrosion initiation and propagation through the remainder of the web depth. Consequently, this paper advocates for a more nuanced approach to modelling corrosion instead of the conventional uniform thickness reduction to encompass the complex geometries associated with localized corrosion. This work investigates the effects of nonuniform corrosion patterns on the web bearing capacity of steel I-girders utilizing finite element modelling, focusing on critical geometric parameters such as corrosion depth, length, and thickness loss. Additionally, the transition of buckling modes is analyzed, offering insights into the necessary considerations for developing effective retrofit strategies that address alternate load paths for vulnerable failure modes. This study aims to enhance the understanding of the residual capacities of deteriorating steel beams and inform better maintenance practices.

1. Introduction

A common cause for the deterioration of steel beams over time is environmental factors, such as corrosion. Corrosion manifests in several forms, such as uniform corrosion, pitting corrosion, and galvanic corrosion. Surface corrosion is the most common form of corrosion. Pitting corrosion, characterized by localized material loss, poses risks because it often extends deeply into the section with minimal visible evidence. Galvanic corrosion typically occurs when dissimilar metals are in contact. Surface corrosion results in a loss of cross-sectional area, leading to a reduction in geometric properties like section modulus and slenderness ratio. Thus, corrosion is detrimental to the load-carrying capacity of structural members in tension, compression, flexure, bearing, and fatigue.

[1] Technical Engineer-I, Hilti Technology Solutions India, <ashrithaiith@gmail.com>
[2] Associate Professor, Indian Institute of Technology Madras, <lakshmipriya@civil.iitm.ac.in>

Moisture often accumulates at the bottom web-flange junction, where corrosion initiates and then propagates through the depth of the cross-section. Corrosion also occurs in the top flange and the top part of the web, but the material loss in these regions is much less than in the web's bottom part. Research by Kayser & Nowak (1989a) indicates that the material loss in the web is more significant than in the flanges, resulting in a greater effect on the reliability of corroded beams in shear and bearing than in flexure. Kayser & Nowak (1989b) showed that the loss of flexural stiffness and strength due to corrosion was linearly proportional to the sectional loss. Likewise, for shear, they observed that the corrosion (typically more severe near the supports) linearly diminishes the shear capacity until the onset of buckling, after which the strength deteriorates rapidly. They further stated that beams that may not have demanded bearing stiffeners at the time of original design may require stiffening after severe corrosion.

Corrosion can alter the failure mode from one to another, with sectional loss potentially lowering the cross-section classification from plastic to compact, semi-compact (noncompact), or slender (Sharifi & Rahgozar 2010a, 2010b, 2010c). A relationship associating the remaining capacities of different failure modes and the thickness loss due to uniform corrosion was proposed in (Sharifi 2012a, 2012b). It provided insight into the relationship between the extent of corrosion and the corresponding remaining structural capacity. This paper utilizes uniform corrosion decay models, which, while conservative, aims to enhance the prediction of service life and the remaining capacity of deteriorating I-beams.

This paper focuses on the loss of bearing capacity in webs because of corrosion. Numerous investigations have established that section loss resulting from corrosion at girder ends can lead to local buckling and crippling in the web and stiffener plates, significantly diminishing the girder's bearing strength. Zmetra et al. (2017) observed that a 70% reduction in web thickness resulted in a 76% decrease in the bearing strength. A web bearing strength reduction factor was proposed by Bao et al. (2021) for different levels of corrosion for evaluating the web bearing strength capacity of corroded steel I-girders to the existing bridge load rating practice adopted in the United States of America. Web bearing buckling happens due to the increased depth-to-thickness ratio as the thickness is reduced because of the corrosion. They showed that the residual web bearing strength of the steel I-girders correlates to the cube of the web thickness and recommended web bearing strength reduction factors to account for different levels of web thinning.

Additionally, pitting corrosion, conceptualized as a rectangular section loss in the form of holes, diminishes the web's cross-sectional area, contributing to reductions in web bearing strength. The reduction in the web bearing strength is more pronounced when the area loss extends parallelly to the girder's longitudinal direction rather than vertically.

Several researchers have devised analytical and practical methods to retrofit corroded girders to regain their original capacity (Goto & Kawanishi, 2004; Mash et al., 2023; Zmetra et al., 2017). Nonetheless, most existing research has modelled corrosion as uniform thickness reduction for estimating the residual bearing strength of steel girders. This approach potentially leads to results that are not realistic. Localized corrosion has complex patterns that significantly impact the bearing capacity of the steel girders. In order to accurately estimate the bearing capacities, these complex geometries of corrosion need to be considered.

The primary objective of this work is to investigate the impact of nonuniform surface corrosion patterns on the web bearing capacity of steel I-girders by finite element modelling (FE). This paper examines the critical geometric parameters, such as corrosion depth, corrosion length and loss of thickness. Furthermore, it discusses the transition of buckling modes from web buckling to crippling and shear buckling. Understanding these phenomena is vital for developing appropriate retrofit strategies that account for alternate load paths associated with the vulnerable failure modes.

2. Finite Element Modelling

This work is performed on a doubly symmetric I-section with compact flanges and web, as per CEN (2022), to preclude local buckling of web or flanges due to flexural compression. The I-section flanges are 300 mm wide and 20 mm thick, while the web is 860 mm deep and 12mm thick. The length of the girder is 12 m. Eigen buckling analyses are conducted in this paper using the FE software (ABAQUS, 2023).

2.1 Mesh elements and mesh discretization

The choice of solid or shell elements in the girder modelling is based on investigations by prior researchers as well as validation studies presented in this paper. Given that FE formulations for solid elements are typically more time-consuming than those for shell elements, it is necessary to compare the simulation results of damage due to local corrosion utilizing both solid and shell elements to evaluate their impact on the buckling modes and ultimate strengths. Khurram et al. (2016) compared the shell and shell-solid coupling FE simulation techniques to understand the effect of uniform and nonuniform local corrosion damages at the bearing stiffener and the adjacent web on the plate girder's overall bearing capacity. Through verification with experimental results comparing the ultimate load, load-displacement curves, and failure patterns, they found that shell elements behaved similarly in both uniform and nonuniform damage. On the other hand, due to the confinement effect available in solid element formulation on both sides, the uniform damage produced marginally greater ultimate capacities than those from nonuniform damage. A solid element provides some extra ductility and post-buckling strength due to plastic deformation induced by minor damage. They concluded that a fine-mesh shell element formulation could be adopted to assess relatively extensive corrosion damage cost-effectively.

This paper presents the results of analyses of a full-sized I-girder to study the web buckling behavior of a steel girder. A reduced integration four-node shell element, S4R, in ABAQUS, (2023) is used to model both flanges and the web of the I-section. The web depth and the flange widths are discretized into 40 and 12 elements, respectively. The validation studies are presented in Section 2.4. The aspect ratio of the web elements is approximately equal to one. The web plate is divided into several subpanels, each of which is assigned a different thickness depending on the corrosion pattern being studied.

2.2 Material Modelling

The paper presents the effects of corrosion on structural steel I-girders, which have an elastic modulus of 200GPa and a Poisson's ratio of 0.32. The yield strength is inconsequential in elastic buckling analyses.

2.3 Loading and Boundary Conditions

Fig. 1 shows the schematic of the 12 m long simply supported beam supported on 1m long bearings at the two ends. The beam is subjected to a uniformly distributed load on the top flange, with top and bottom flange lateral braces (fully effective torsional braces) placed at 2m intervals along the beam length to prevent lateral torsional buckling (LTB) failure, ensuring that the beam would primarily fail by web bearing. Flange corrosion effects are not a part of the studies presented in this paper to isolate the specific effects of web corrosion on the residual web bearing capacity.

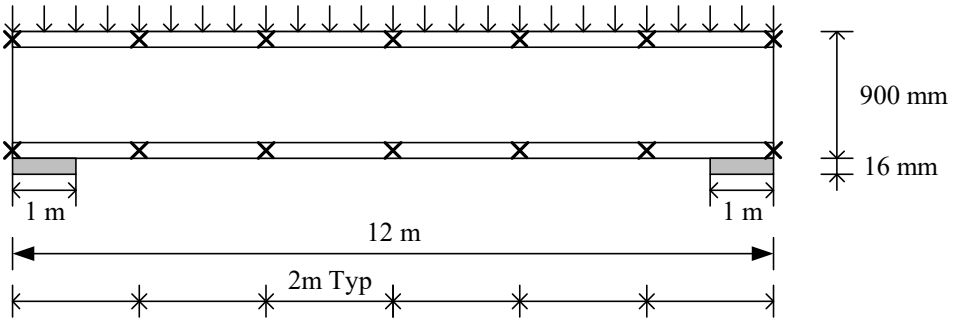

Figure 1: Schematic of a simply supported beam supported on bearings and subjected to a uniformly distributed load

The steel bearing plate is also modelled using shell elements, which share the mesh size throughout the length of the bearing plate. It has a bearing length of 1 m and a bearing thickness of 16 mm. A tie constraint is exercised between the bearing plate and the bottom of the flange that is restrained against vertical displacement, facilitating the accurate simulation of the support reaction. This constraint ensures that the interactions between the bearing plate and the flange are well-defined and realistic. The boundary conditions are simulated with one bearing plate under the bottom flange as pinned and at the other end as roller support. The lateral displacements of the web at the ends are restricted, effectively restraining the twist of the beam at its ends.

2.4 Validation of the FE model

This section presents a validation of the current FE model with the results presented by Bao et al. (2021) for an I-girder with uniform web thinning. Fig. 2 shows the FE model generated in ABAQUS (2023) considering uniform web thinning. It also shows the web buckling mode of a 20% corroded specimen obtained by eigenvalue buckling analysis. Fig. 3 compares the benchmark study with the FE simulation results for the web bearing strength, where the horizontal axis denotes the percentage of web loss, and the vertical axis specifies the remaining percentage of the girder's original web buckling strength.

The validation studies show excellent agreement with the results presented by Bao et al. (2021) and the FE models using the mesh discretization and materials defined in the preceding sections of this paper. However, this paper focuses on the behavior of I-girders undergoing nonuniform surface corrosion. Fig. 4 shows the FE model developed in the current study for analyzing nonuniform corrosion.

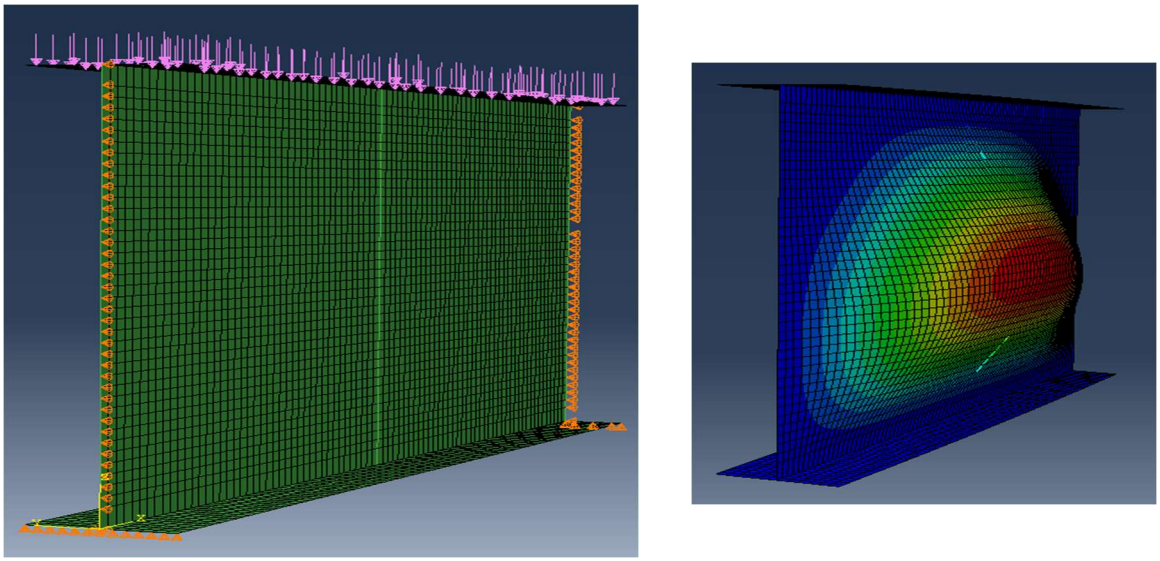

Figure 2: Finite element model of the beam in ABAQUS (left) and the web buckling mode of a 20% corroded beam specimen (right).

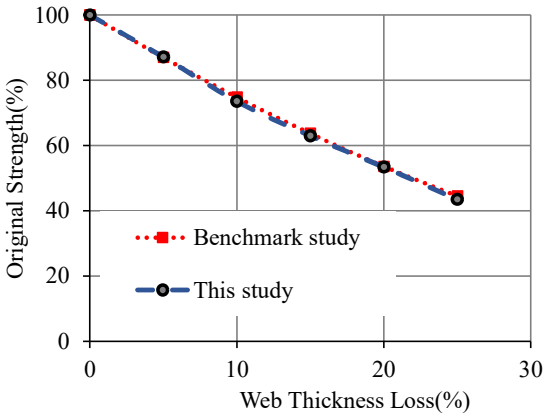

Figure 3: Comparison of the I-girder residual web bearing strength with uniform web thinning in the benchmark study (Bao et al. 2021) and the FE validation studies.

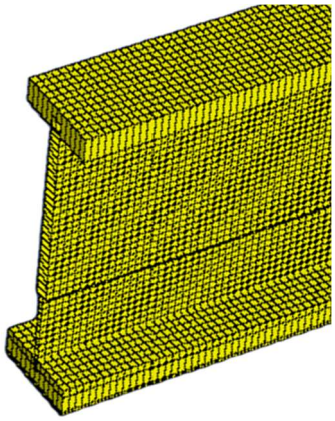

Figure 4: Finite element model for understanding nonuniform corrosion effects.

3. Parametric Studies for nonuniform corrosion

With the help of the validated FE model described in Section 2, the behavior of the corroded I-beam is investigated for two corrosion patterns, illustrated in Fig. 5.

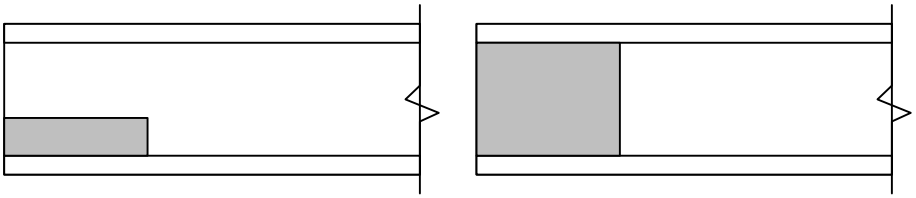

Figure 5: Nonuniform corrosion patterns: Pattern 1 (left) and Pattern 2 (right) (adapted from Tzortzinis et al. 2019).

3.1 Corrosion Patterns

The studies presented in this paper consider a rectangular area of deterioration, referred to as Patterns 1 and 2. The parameters of *Pattern 1* are listed below with respect to the web depth, d_w and web thickness, t_w.

Corrosion Height (CH) = [0.1-0.3] times of d_w

Corrosion Length (CL) = [0-1.5] times of d_w

Thickness of the corroded portion = [5-80] % of t_w

A parametric study is conducted to analyze the effects of varying corrosion heights, corrosion lengths and thickness loss on the bearing capacity of the girder. This study examines corrosion heights at $0.1d_w$, $0.2\ d_w$ and $0.3d_w$ in conjunction with different corrosion lengths at varied intervals. The corrosion depth is restricted to $0.3d_w$ based on the findings reported by Yao et al. (2022).

The parameters of *Pattern 2* are:

Corrosion Height (CH) = [1] times of d_w

Corrosion Length (CL) = [1.0 – 1.5] times of d_w

Thickness of the corroded portion = [5-80] % of t_w

A parametric study is conducted to analyze the effects of varying corrosion heights, and thickness loss on the bearing capacity of the girder with pattern 2 corrosion. The study examines corrosion lengths of 1 d_w, 1.1 d_w, 1.2 d_w, 1.3 d_w, 1.4 d_w and 1.5 d_w.

3.2 Effect of Corrosion Length

The FE test simulation results for the range of upper and lower bounds of the geometric dimensions listed in Section 3.1 are presented here, emphasizing the effect of corrosion length on the web bearing strength. The FE models assume a uniform thickness reduction across the corroded area, with the full web thickness in the remaining web areas.

Fig. 6 presents the effects of corrosion lengths varying from 10% to 150% of the web depth on the bearing capacity of the beam, which is equivalent to 10% to 132% of the bearing length. The material losses range from 5% to 80% of the original web thickness, as depicted in Pattern 1. The corrosion heights are set at 10%, 20% and 30% of the web's depth**.** Additionally, the figures include the strength losses due to uniform corrosion across the web to enable a comparative analysis with localized corrosion effects.

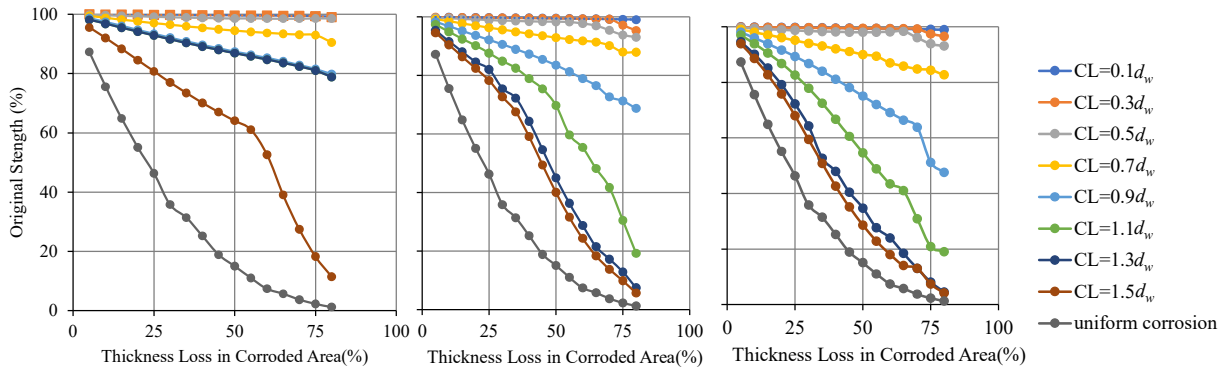

(a) (b) (c)

Figure 6: Effect of corrosion length for corrosion heights of (a) 10% (b) 20% (c) 30% of the web depth on the I-plate girder bearing capacity in Pattern 1.

The following may be gleaned from Fig. 6:

1. Fig. 6 illustrates the impact of different corrosion lengths on the bearing capacities for each corrosion height. Clearly, an increase in corrosion length results in a decrease in the bearing capacity.
2. For a given corrosion depth, the bearing strength decreases almost linearly with an increase in section loss. However, for a corrosion length of $1.5d_w$ and a corrosion depth of $0.1d_w$, the failure mode changes from local buckling to crippling at 55% section loss, resulting in a bi-linear curve. The rate of capacity decrease accelerates once crippling initiates.
3. An increase in corrosion depth from $0.1d_w$ to $0.2d_w$ triggers web crippling at lower corrosion lengths.
4. There is negligible effect on the bearing capacity when the corrosion lengths exceed the bearing lengths for corrosion depths of $0.2d_w$ and $0.3d_w$.

Fig. 7 illustrates the impact of different corrosion lengths of 100%, 110%, 120%, 130%, 140% and 150% of the web depth, which correspond to 88%, 96.8%, 105.6%, 114.4%, 123.2% and 132% of the bearing length respectively. The material losses range from 5% to 80% of the original web thickness, as depicted in corrosion Pattern 2 on the web bearing capacity.

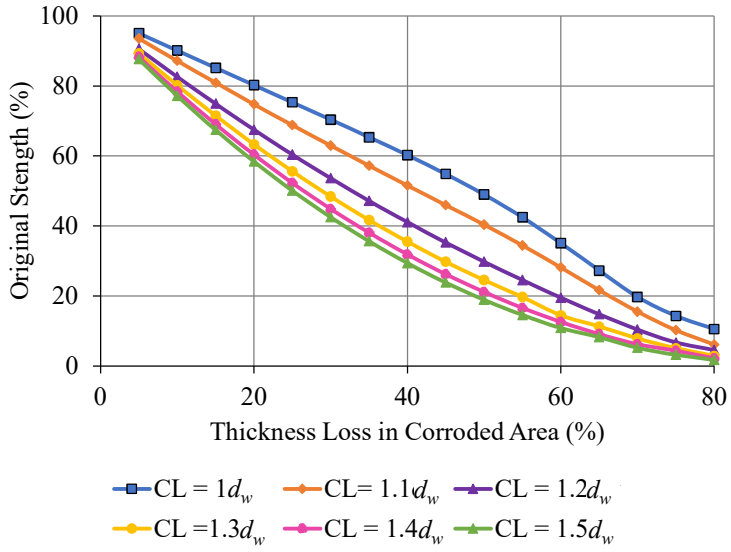

Figure 7: Variation in residual web bearing capacity with web thickness loss for different corrosion depths for Pattern 2.

Fig. 7 shows that the bearing capacity decreases with increased corrosion length, as in Pattern 1. Further, there is no significant impact on the bearing capacity when the corrosion length exceeds 130% of the web depth, and it is safe to conclude that for corrosion lengths greater than the bearing length, its impact on the bearing capacity decreases, and the effects of section loss dominate.

Fig. 8 shows the typical failure modes identified for Pattern 2 corrosion for two different corrosion lengths - 150 and 110% of the web depth (132% and 98% of the bearing lengths).

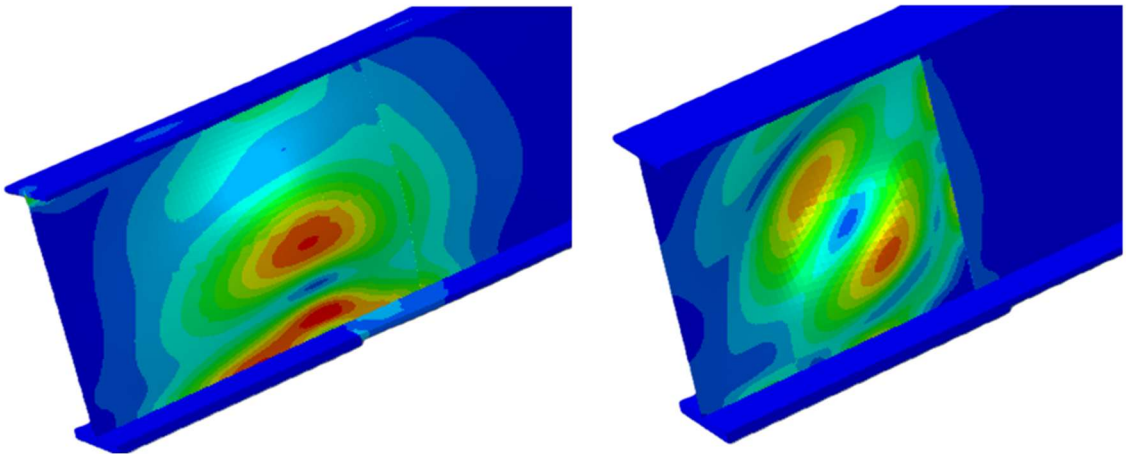

Figure 8: Typical failure modes for corrosion Pattern 2: (a) For corrosion length of 1.5 times the web depth (132% of the bearing length) and (b): For corrosion length of 1.1 times the web depth (97% of the bearing length).

Interestingly, Fig. 8 suggests that diagonal web shear buckling occurs when the corrosion length nearly equals the bearing length for higher thickness losses through the web depth.

3.2 Effect of Corrosion Depth

Fig. 9 illustrates the impact of corrosion heights (10%, 20% and 30% of the web's depth) of Pattern 1 on the web bearing capacity. The corrosion lengths are set at specific values: 30%, 70%, 90%, 110%, 130% and 150% of the depth, corresponding to 8.8%, 61.6%, 79.2%, 96.8%, 114.4% and 132% of the bearing length.

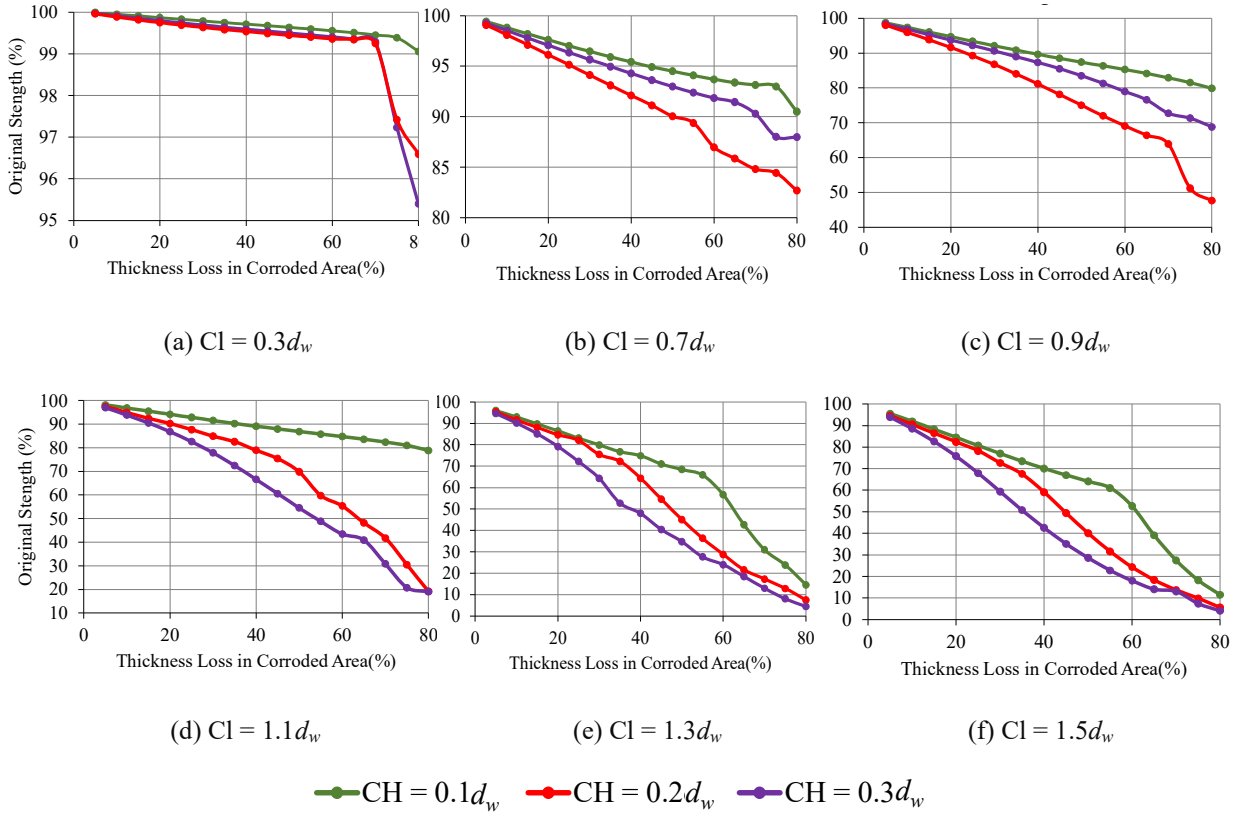

Figure 9: Effect of corrosion depth (CH) on the web bearing capacity for different levels of material loss.

Fig. 9 shows that the bearing capacity decreases with an increase in corrosion height. Where the curves change slope, the failure mode changes from web buckling to crippling. As before, the strength deterioration is faster once crippling begins.

3.2 Effect of loss of web thickness

Fig. 10 illustrates the failure modes for Pattern 1, which shows that the buckling is confined to the corroded areas in cases where the material is significantly reduced, with the buckling wave forming only along the height of the corroded region. Hence, as the thickness loss progresses, the failure mode transitions from local buckling to crippling. This progression highlights how the bearing capacity is compromised in different stages of material degradation.

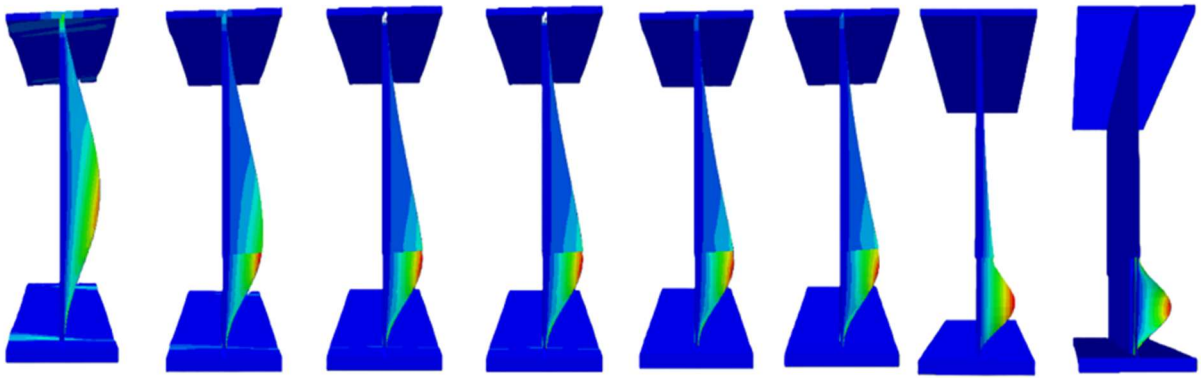

Figure 10: The failure modes for a corrosion height of $0.3d_w$ and a corrosion length of 1.5 d_w transitioning from web buckling to web crippling with increasing thickness loss from left to right

4. Conclusions

This paper examines the role of corrosion height, length and thickness loss on the residual web bearing capacity of steel I-beams and shows the importance of modelling nonuniform web thinning by illustrating the change in the buckling modes for different sectional losses. Failures can manifest as web buckling, web crippling, or diagonal shear buckling, depending on the specific combination of corrosion parameters. Through finite element simulations, this paper concludes the following:

1. For smaller corrosion depths, the buckling mode shifts from a web buckling to a web crippling mode at over 50% section loss, after which the strength deteriorates rapidly. Conversely, an increase in corrosion depth instigates web crippling at smaller corrosion lengths.
2. Bearing capacity is not greatly affected when corrosion lengths exceed the bearing length.
3. Increasing thickness loss alters the buckling mode from web buckling to crippling.
4. Web shear buckling is observed when the corrosion length is approximately equal to the bearing length for higher thickness losses when the entire web depth is corroded.

The findings presented in this paper indicate that a substantially greater understanding of the influence of various geometric parameters on the web bearing strength is required, and the necessity for more accurate modelling techniques than uniform web thinning considerations. Such studies will enable a more rational approach to repair and retrofit corroded steel I-beams.

Acknowledgments

This work was supported by the Science and Engineering Research Board, India.

References

ABAQUS. (2023). [Computer software]. Dassault systémes, Waltham, MA.

Bao, A., Guillaume, C., Satter, C., Moraes, A., Williams, P., Kelly, T., & Guo, Y. (2021). “Testing and evaluation of web bearing capacity of corroded steel bridge girders.” *Engineering Structures*, 238(July). https://doi.org/10.1016/j.engstruct.2021.112276

CEN (2022). Eurocode 3: Design of steel structures - Part 1-1: General rules and rules for buildings, EN 1993-1-1:2022 (E), CEN (European Committe Stand. Brussels, Belgium 1–120.

Goto, Y., & Kawanishi, N. (2004). “Analysis to predict long-term mechanical performance of steel structures with histories of corrosion and repair.” *Journal of Structural Engineering*, 130(10), 1578–1585. https://doi.org/10.1061/(ASCE)0733-9445(2004)130

Kayser, J. R., & Nowak, A. S. (1989a). “Capacity loss due to corrosion in steel-girder bridges.” *Journal of Structural Engineering*, 115(6), 1525–1537.

Kayser, J. R., & Nowak, A. S. (1989b). “Reliability of corroded steel girder bridges.” *Structural Safety*, 6(1), 53–63. https://doi.org/10.1016/0167-4730(89)90007-6

Khurram, N., Sasaki, E., Akmal, U., Saleem, M. U., & Amin, M. N. (2016). “A comparative study in utilizing the shell and solid elements formulation for local corrosion simulation at bearing stiffener.” *Arabian Journal for Science and Engineering*, 41, 3897–3909. https://doi.org/10.1007/s13369-015-2018-x

Mash, J. A., Harries, K. A., & Rogers, C. (2023). “Repair of corroded steel bridge girder end regions using steel, concrete, UHPC and GFRP repair systems.” *Journal of Constructional Steel Research*, 207(April), 107975. https://doi.org/10.1016/j.jcsr.2023.107975

Sharifi, Y., Rahgozar, R. (2010a). “Evaluation of the remaining shear capacity in corroded steel I-beams.” *International Journal of Advanced Steel Construction*, 6(2), 803–816

Sharifi, Y., Rahgozar, R. (2010b). “Remaining moment capacity of corroded steel beams.” *International Journal of Steel Structures*, 10(2), 165–176

Sharifi, Y., Rahgozar, R. (2010c). “Simple assessment method to estimate the remaining moment capacity of corroded I-beam sectionss.” *Scientia Iranica Journal*, 17(2), 161–167

Sharifi, Y. (2012a). “Residual web bearing capacity of corroded steel beams.” *Advanced Steel Construction*, 8(3), 242–255.

Sharifi, Y. (2012b). “Uniform Corrosion wastage effects on the load-carrying capacity of damaged steel beams.” *Advanced Steel Construction*, 8(2), 153–167.

Tzortzinis, G., Gerasimidis, S., Brena, S., & Knickle, B. (2019). “Development of load rating procedures for deteriorated steel beam ends: Deliverable 4 (Issue 19).” University of Massachusetts at Amherst, Massachusetts Department of Transportation Office of Transportation Planning.

Yao,Y., Fu,Z., Jia,B., and Wan,L., (2022), “Buckling and Bearing Capacity Variation caused by Local Corrosion at Support in Steel Bridge,” *KSCE Journal of Civil Engineering*, 26(11), 4573-4583

Zmetra, K. M., McMullen, K. F., Zaghi, A. E., & Wille, K. (2017). “Experimental study of UHPC repair for corrosion-damaged steel girder ends.” *Journal of Bridge Engineering*, 22(8), 1–14. https://doi.org/10.1061/(asce)be.1943-5592.0001067